High Impedance Surface Application to Dipole Antenna Design

Samir Berkani [1], Youssef Lamhene [1], Mustapha Hadj-Sadok [1], and Henri Baudrand [2]

[1] Laboratoire d'Instrumentation, FEI, Université USTHB, Alger
sam-30@live.fr, lamhene.y@gmail.com, mustaphahadjsadok@gmail.com

[2] Laboratoire RCEM, Toulouse, France
henri.baudrand@yahoo.fr

Abstract ─ in this paper, HIS (High Impedance Surface) are used, in order to verify their utilities; we have considered two different structures as a ground. The first is mushroom EBG (Electromagnetic Band Gap) structure which is composed of several patches with a ground connecting via, where the second is 2D metamaterial structure with resonant rings. Both the structures are investigated by simulation and compared at the frequency 12 GHz. The metamaterials proprieties are successfully verified around the resonant frequency.

Index Terms ─ Digital capacitance, EBG structures, metamaterials, negative index materials, wire antenna.

I. INTRODUCTION

The antennas manufacture requires a big precision in realization, because the dimensions of these circuits are of the same order of magnitude as the wave length. Considering imprecision factors due to the manufacture constraint, surface waves will be engendered; consequently, antenna performance will be influenced.

A special material is used to block surface waves known as metamaterial, it enhances significantly the antenna performance which is characterized by simultaneously negative values of the permeability and the permittivity [1]; it doesn't exist in natural state.

Metamaterials enhance significantly the antenna performance. They have interesting proprieties [2], it consists in stopping surface waves to propagate along the surface, there is no phase delay to be introduced to the progressive wave and the evanescent wave is amplified. Hence, we can say that both propagating and evanescent waves contribute to the resolution of the system and circuit's spatial frequency is restored. Therefore the wave behaves as there is no physical obstacle [3-4].

II. METAMATERIAL TRANSMISSION LINE THEORY

Figure 1 [5] shows a cell of metamaterial transmission line which is a combination of Right-Handed Transmission Line (RHTL) and Left-Handed Transmission Line (LHTL). By applying the Kirchhoff law, it results:

$$\begin{cases} \dfrac{\partial v(x,t)}{\partial x} = Zi(x,t) = j\left(L_R.\,\omega - \dfrac{1}{\omega.\,C_L}\right) i(x,t), & (1) \\ \dfrac{\partial i(x,t)}{\partial x} = Yv(x,t) = j\left(C_R.\,\omega - \dfrac{1}{\omega.\,L_L}\right) v(x,t). & (2) \end{cases}$$

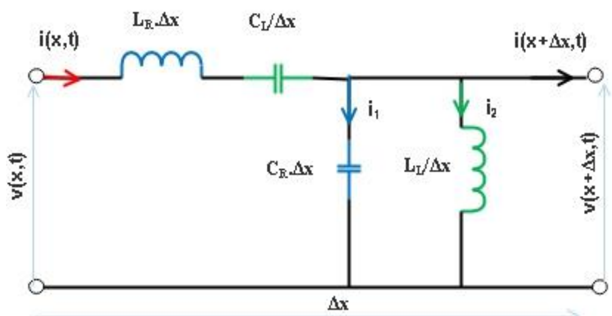

Fig. 1. Metamaterial transmission line cell model.

We solve simultaneously (1) and (2), we obtain the wave equations, for Voltage wave V:

$$\partial^2 v(x,t)/\,\partial x^2 = -Z\,Yv(x,t) = -\gamma^2 v(x,t). \quad (3)$$

Where:

$$\gamma = \sqrt{Z\,Y} = \alpha + j\beta = \sqrt{-\omega^2(L_R C_R + \frac{1}{(\omega^2\sqrt{L_L C_L})^2} - \frac{L_R C_L + L_L C_R}{(\omega\sqrt{L_L C_L})^2}}\,. \quad (4)$$

We can introduce the RH resonant frequency: $\omega_R = \frac{1}{\sqrt{L_R C_R}}$. And LH resonant frequency $\omega_L = \frac{1}{\sqrt{L_L C_L}}$, it results:

$$\gamma = j\sqrt{(\omega/\omega_R)^2 + (\omega_L/\omega)^2 - k\omega_L^2}\,. \quad (5)$$

Equation (5) describes all the behaviors of the metamaterial transmission line.

Figure 2 shows the graph of the complex propagation constant. Where A = max($\boldsymbol{\omega_s}, \boldsymbol{\omega_P}$), B = min($\boldsymbol{\omega_s}, \boldsymbol{\omega_P}$) and C = ω_F, ω_s, ω_P and ω_F are respectively the series, shunt resonance frequencies and maximum attenuation frequency [5].

Submitted On: March 10, 2018
Accepted On: April 3, 2019

We consider Fig. 2, if $\omega < \min(\boldsymbol{\omega_s}, \boldsymbol{\omega_P})$, the phase velocity (slope of the line segment from origin to curve) and group velocity (slope of the curve) have opposite sign (they are antiparallel) which means that the transmission line is left-handed and that β is therefore negative.

If we apply Maxwell equations and use (1) and (2), it results:

$$\begin{cases} \mu(\omega) = L_R - \dfrac{1}{\omega^2 C_L}, & (6) \\ \varepsilon(\omega) = C_R - \dfrac{1}{\omega^2 L_L}. & (7) \end{cases}$$

When $\omega << \min(\boldsymbol{\omega_s}, \boldsymbol{\omega_P})$, (6) and (7) become:

$$\begin{cases} \mu(\omega) = -1/\omega^2 C_L < 0 \\ \varepsilon(\omega) = -1/\omega^2 L_L < 0 \end{cases} \text{Left-Handed Transmission Line.}$$

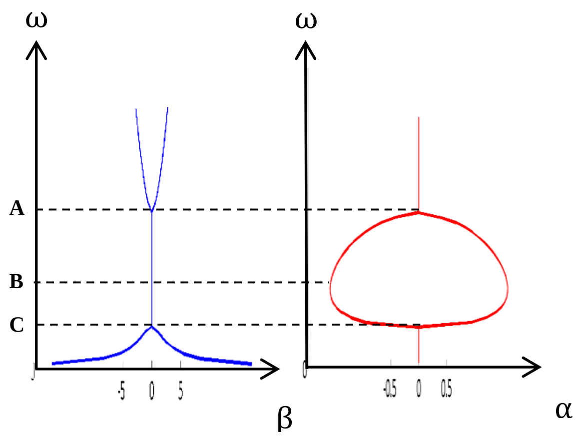

Fig. 2. Complex propagation constant vs. frequency

III. SIMPLE DIPOLE ANTENNA RESPONSE

Figure 3 shows the radiation pattern of dipole antenna in free space. In horizontal plane (3.B), when viewed from above, the pattern exhibits two lobes which represent the omnidirectional characteristic of the dipole antenna (bidirectional radiation).

When a dipole antenna is installed close to the earth's surface, the pattern radiation is attenuated because of the reflection from the surface [6]. In the ideal case, the gain of the dipole antenna doesn't exceed 3 dB as shown on Fig. 4.

IV. MODELS AND DIMENSIONS

In order to investigate the performance of the dipole antenna, it will be installed close to different surfaces and each structure will be also optimized in order to seek the best results.

A. Dipole above a perfect electric conductor (PEC)

The most simple structure is a ground plane placed under the dipole antenna (27.5X27.5 mm) of distance h_{dist} = 1.925 mm functions as reflector as shown on Fig. 5.

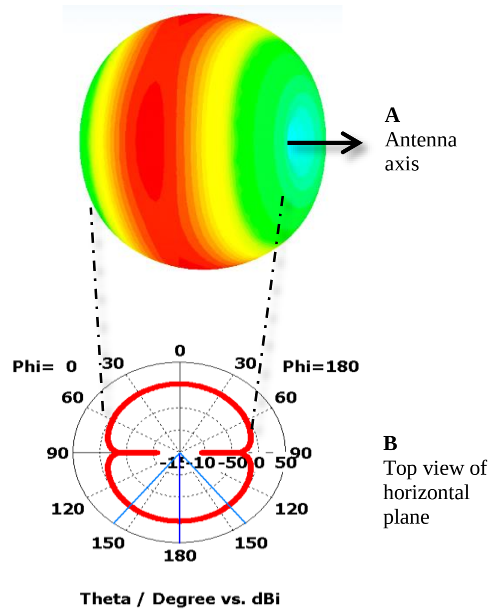

Fig. 3. Idealized dipole radiation pattern.

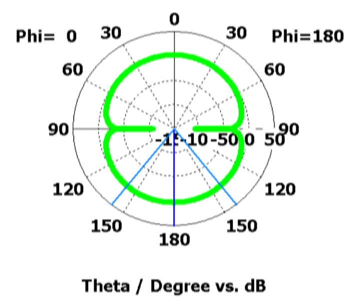

Fig. 4. Dipole radiation diagram of the gain at 12 GHz.

Fig. 5. Dipole antenna above a reflector.

B. Dipole above EBG substrate (mushroom)

The second model is the dipole antenna placed above EBG substrate of distance h_{dip} = 0.02λ. It is composed of several patches of side width w = 0.12λ, gap width g = 0.02 λ, substrate thickness h = 0.04 λ and via hole of ray r = 0.005λ.

We have considered the following parameters as: dipole length L = 0.452λ and dielectric constant ε_r = 2.17 for the frequency 12 GHz (red graph in Fig. 10), the dipole length L = 0.457λ and dielectric constant ε_r = 2.2 for the frequency 12.228 GHz (green graph in Fig. 10). Figure 6 illustrates the model.

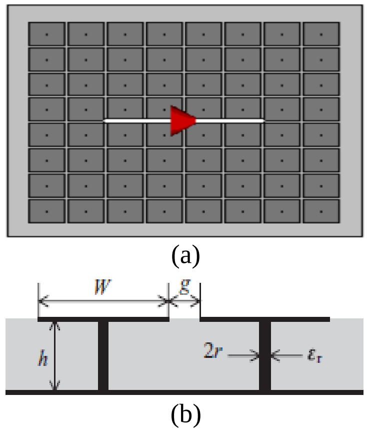

Fig. 6. (a) Dipole antenna above mushroom structure, and (b) parameters of mushroom cells.

C. Dipole antenna above 2D structure substrate with digital capacitors and rings

The third model is the dipole antenna placed above substrate of distance h_{dip} = 0.02λ, permittivity ε_r = 2.2 and thickness h = 1.25 mm. It is composed of several patches of width w_{patch} = 0.084λ, seven digits digital capacitors of parameters w_{digit} = 0.0084λ and rings with parameters: r_{ring} = 0.08λ [7], a = 0.007λ, the space between rings g = 0.02 λ and via hole of ray r = 0.005λ.

We have considered the digit length of the digital capacitor (L_{digit}) and the dipole length (L) as follows:

L_{digit} = λ/4 and L = 0.41λ;

for the frequency 12 GHz (red graph in Fig. 12):

L_{digit} = λ/5 and L = 0.42λ;

for the frequency 11.772 GHz (green graph in Fig. 12).

Figure 8 illustrates the model, where the digital capacitor as shown on Fig. 7 can be calculated by the following formula [8]:

$$C\left({}^{pF}/_{\mu m}\right) = (\varepsilon_r + 1)l[(N-3)A_1 + A_2]. \quad (8)$$

Such as:

$$A_1 = 4.409 \tanh\left[0.55\left({}^{h}/_{W}\right)^{0.45}\right]10^{-6}, \quad (9.a)$$

$$A_2 = 9.92 \tanh\left[0.52\left({}^{h}/_{W}\right)^{0.5}\right]10^{-6}. \quad (9.b)$$

Where W = S = S’, N is the number of digits.

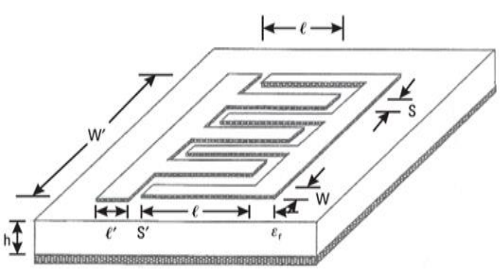

Fig. 7. Seven digits of the digital capacitor.

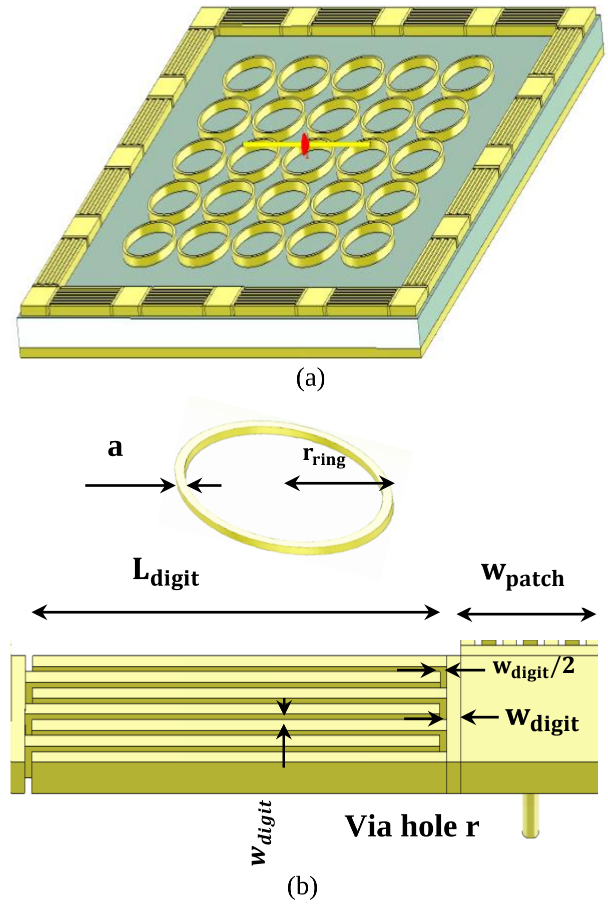

Fig. 8. 2D structure with digital capacitor and rings: (a) structure and (b) parameters.

V. RESULTS

The return loss of the first model as shown on Fig. 9 below doesn’t satisfy the minimum attenuation, it can’t be used as a ground.

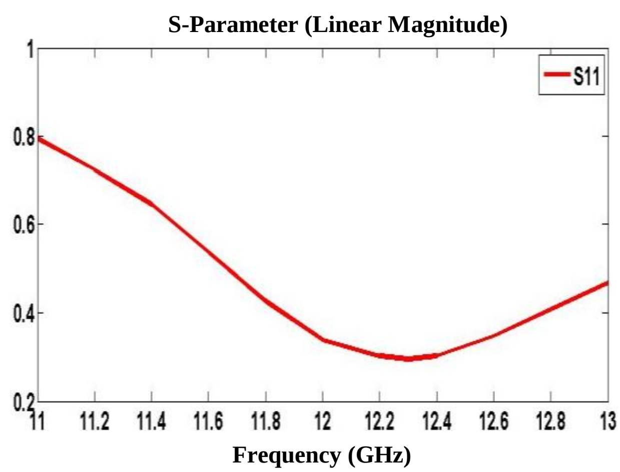

Fig. 9. Return loss vs. frequency of the dipole above PEC ground.

Figure 10 shows the graph of the reflection coefficient dipole antenna above mushroom structure. Two different graphs appear: we have considered the dipole length L = 0.452λ and ε_r = 2.17 for the red graph, the dipole length L = 0.457λ and ε_r= 2.2 for the green graph.

From the curve it's clear that the antenna at 12.228 GHz reaches a perfect resonance, it has the minimum value of the reflection coefficient -41.39 dB compared to 12 GHz operating frequency which has less reflection -26.45 dB.

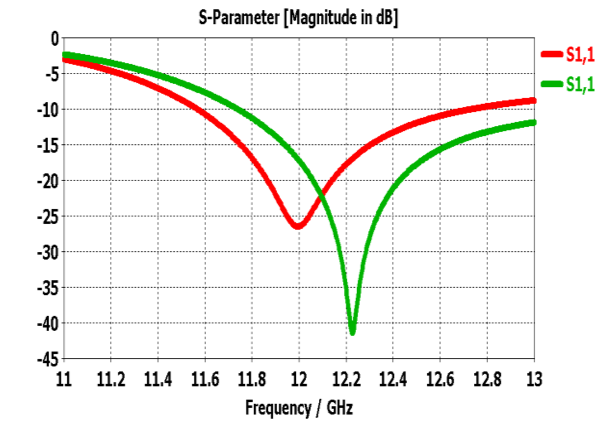

(a)

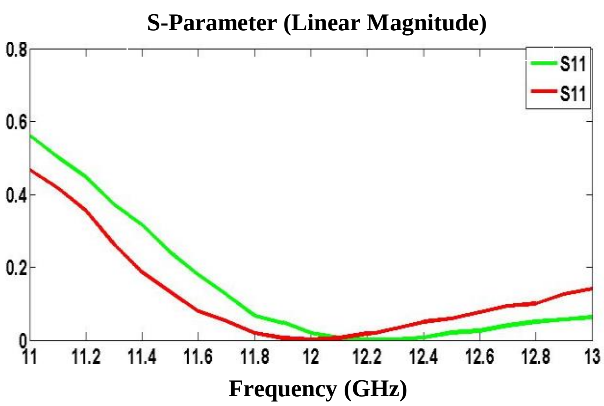

(b)

Fig. 10. Dipole mushroom return loss for 12 GHz operating frequency and around: (a) magnitude in dB and (b) linear magnitude.

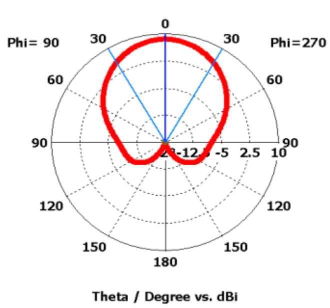

(a)

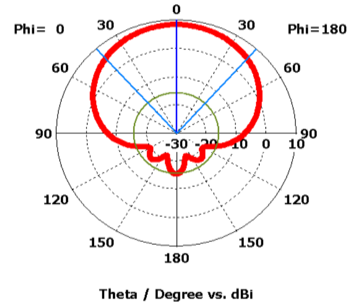

(b)

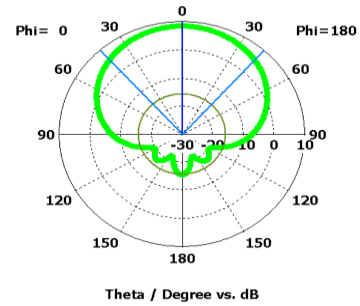

(c)

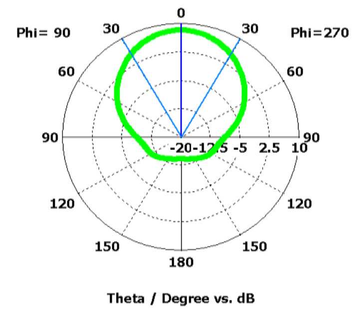

(d)

Fig. 11. Dipole mushroom parameters: (a) directivity at 12.228 GHz, (b) directivity at 12 GHz, (c) gain at 12 GHz, and (d) gain at 12.228 GHz.

Figure 11 shows the different parameters of the dipole mushroom structure, the graphs show that the gains are closely similar at 12 GHz and 12.228 GHz, they reach 8.3 dB, but the structure is more directive at 12.228 GHz, 59.8 deg. compared to 83.5 deg. at 12 GHz.

Figure 12 shows the graph of the reflection coefficient dipole antenna above 2D structure with digital capacitors and rings. Two different graphs appear: we have considered L_{digit} = λ/4 and the dipole length L = 0.41λ for the red graph, L_{digit} = λ/5 and the dipole length L = 0.42λ for the green graph.

Compared to the mushroom structure, we have more reflection at 12 GHz and also around the resonant frequency: -30 dB at 12 GHz and -45 dB at 11.772 GHz.

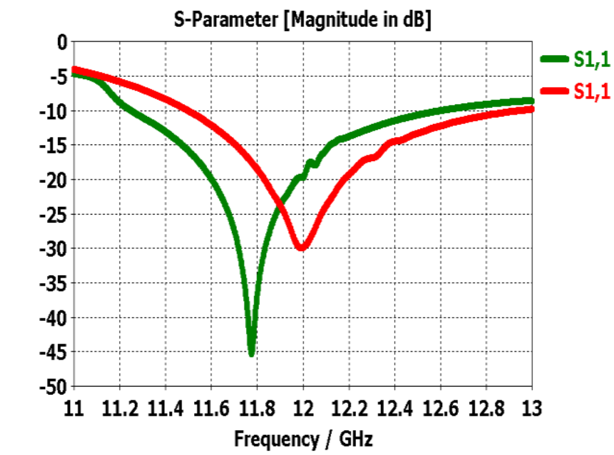

(a)

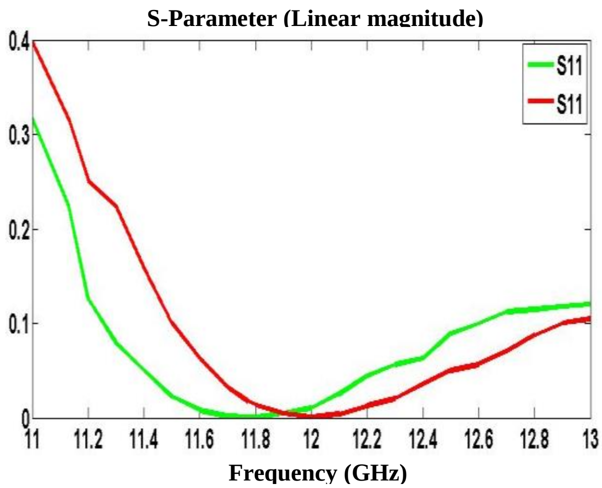

(b)

Fig. 12. Dipole above 2D structure with digital capacitors and rings: return loss for 12 GHz operating frequency and around.

Furthermore, the gain is increased by 1 dB at 12 GHz and close to 2 dB around the resonant frequency as shown on Fig. 13. As for the directivity, we obtain 59.4 deg. at 12 GHz and 56 deg. around the resonant frequency as shown on Fig. 14.

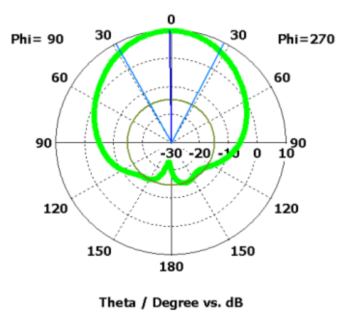

(a)

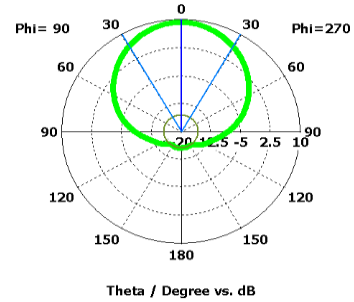

(b)

Fig. 13. Dipole above 2D structure with digital capacitors and rings: (a) gain at 11.772 GHz and (b) gain at 12 GHz.

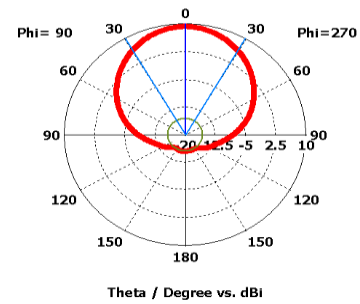

(a)

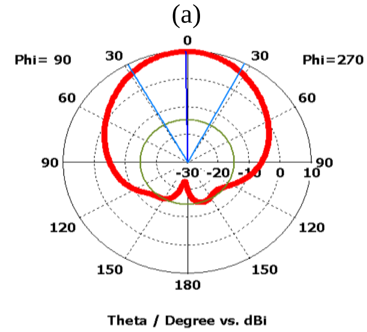

(b)

Fig. 14. Dipole above structure with digital capacitors: (a) directivity at 12 GHz and (b) directivity at 11.772 GHz.

VI. CONCLUSION

Two HIS structures have been simulated and compared to prove the application utility of the metamaterials and verify theirs proprieties. Both the structures considered have successfully enhanced the performance of the dipole antenna, whereas the simple dipole is an omnidirectional antenna, the antennas considered in this article become directives with a much higher gain, close to 10 dB compared to the gain of 2 dB of the simple dipole antenna. These structures have successfully contributed to block surface waves.

We have used the digital capacitor because it allows a greater capacity value than the gap capacitor and combined resonators with 2D metamaterial make the circuit original compared to the classical mushroom.

The results are obtained by using CST which is based on one of the most popular numerical method for the solution of electromagnetic problems (FDTD) [9].

REFERENCES

[1] V. G. Veselago, "The Electronics of Substances with Simultaneously Negative Values of ε and μ," *P. N. Lebedev Physics Institute*, Academy of Science, USSR, Jan.-Feb. 1968.

[2] A. Ben, "Metamaterials Critique and Alternatives," *The Ohio State University*, ed., Wiley.

[3] J. B. Pendry, "Negative Refraction Makes a Perfect Lens, Condensed Matter Theory Group," *The Blackett Laboratory, Imperial College*, London SW7 2BZ, United Kingdom, 30 Oct. 2000.

[4] S. J. Orfanidis, *Electromagnetic Waves and Antennas*, Copyright ©1999-2008.

[5] C. Caloz and T. Itoh, "Electromagnetic Metamaterials: Transmission Line Theory and Microwave Applications: The Engineering Approach," *Ecole Polytechnique de Montréal, University of California at Los Angeles*, ed., Wiley 2006.

[6] J. J. Carr, *Practical Antenna Handbook*, ed., McGraw-Hill, 2001.

[7] I. Tomeo-Reyes and E. Rajo-Iglesias, "Comparative Study on Different HIS as Ground Planes and Its Application to Low Profile Wire Antennas Design," *University Carlos III of Madrid*, Spain, 2011.

[8] I. Bahl, *Lumped Elements for RF and Microwave Circuits*, ed., Artech House, Inc., 2003.

[9] J. B. Schneider, "Understanding the Finite-Difference Time-Domain Method," Jan. 2, 2011.

Samir Berkani is a Ph.D. student in Telecommunication and Microwave at the FEI (Faculté d'Electronique et d'Informatique) and LINS Laboratory (Laboratoire d'Instrumentation), USTHB (Université des Sciences et Technologies Houari Boumediene), he received the diploma of Electronics Dngineer from Saad Dahlab University Blida, Algeria, Faculty of Telecommunications, in 1998, and Magister in rayonment and microwave in USTHB, FEI, Bab ezzouar Algeria, in 2013.

He is working actually on metamaterials applied in antennas design interesting in enhancing gain and directivity, under the supervision of Dr. Y. Lamhene.

Youssef Lamhene received bachelor's degree then master's degree in Electronic, Electrotechnic and Automatic (EEA), in 1978 and 1980 from Lille University in France, and later on, in the same place, the DEA diploma in 1982 and the third cycle Doctorate diploma in Biotechnology domain in 1984. He is also, since 2009, state Doctor of the Houari Boumediène University of Sciences and Technology. He teaches graduate level courses in applied electronic, microwave and antenna theory at the sciences and technology university of Algiers. His research interests are in the area of electromagnetic simulations of microwave and millimeter-wave passive components.

Hadj Sadok Mustapha is a Ph.D. student in Electronique Instrumentation and Optronic Systems at the FEI (Faculty of Electronics and Data processing), in 2014 he received the master's degree from USTHB (University of Science and Technology Houari Boumediene), Algeria, He is working actually on metamaterials applied in antennas design interesting in enhancing gain and directivity, at LINS (Instrumentation Laboratory), under the supervision of Dr. Y. Lamhene.

Henri Baudrand is Emeritus Professor at ENSEEIHT, Toulouse, France. He specializes in modeling passive and active circuits and antennas. He is the author and co-author of three books at Cepadues edition. He has co-authored over 100 publications in journals and 250 contributions to international conferences. He is a Fellow Member of IEEE Society, a Member of "Electromagnetism Academy" and a Senior Member of IEE Society. He was the President of URSI, France Commission B for six years (1993 to 1999) and the President of the IEEE-MTT-ED French Chapter. He was awarded "Officier des Palmes Académiques", and Director Honoris causa of Lasi University.